Journal of Power Sources 195 (2010) 580–587

Contents lists available at ScienceDirect

Journal of Power Sources

journal homepage: www.elsevier.com/locate/jpowsour

Carbonate-modified siloxanes as solvents of electrolyte solutions for rechargeable lithium cells

Takashi Takeuchi, Satoshi Noguchi, Hideyuki Morimoto, Shin-ichi Tobishima*

Department of Chemistry, Faculty of Engineering, Gunma University, Kiryu, Gunma, 376-8515, Japan

ARTICLE INFO

Article history:
Received 18 June 2009
Received in revised form 24 July 2009
Accepted 25 July 2009
Available online 3 August 2009

Keywords:
Lithium cell
Electrolyte
Rechargeable cell
Siloxane
Cell safety
Cycling efficiency

ABSTRACT

Influence of mixing carbonate-modified siloxanes into $LiPF_6$-ethylene carbonate (EC)/ethylmethyl carbonate (EMC) (mixing volume ratio = 3:7) mixed solvent electrolytes on charge–discharge cycling properties of lithium was examined. As the solute, 1 M (M: mol L^{-1}) $LiPF_6$ was used. As siloxanes, 4-(2-trimethylsilyloxydimethylsilylethyl)-1,3-dioxolan-2-one and 4-(2-bis(trimethylsilyloxy)methylsilylethyl)-1,3-dioxolan-2-one were investigated. These siloxanes are derivatives of butylene cyclic carbonate or vinyl ethylene carbonate. Charge–discharge cycling efficiencies of lithium metal anodes improved and an impedance of anode/electrolyte interface decreased by mixing siloxanes, compared with those in 1 M $LiPF_6$-EC/MEC alone. Slightly better cycling behavior of natural graphite anode was obtained by adding siloxanes. Si–C/$LiCoO_2$ cells exhibited better anode utilization and good cycling performance by using 1 M $LiPF_6$-EC/MEC + siloxane electrolytes. Thermal behavior of electrolyte solutions toward graphite–lithium anodes was evaluated with a differential scanning calorimeter. By adding siloxanes, temperature starting the large heat-output of graphite–lithium anodes with 1 M $LiPF_6$-EC/MEC electrolyte solutions shifted to higher temperature about 100 °C. However, amount of heat-output did not decrease by adding siloxanes.

1. Introduction

Many of commercial lithium ion cells are composed of carbon anode and $LiCoO_2$ cathode with nonaqueous electrolyte solutions. Typical example of nonaqueous electrolyte solutions is $LiPF_6$-ethylene carbonate (EC)/methylethyl carbonate (MEC). The improvement of energy density of lithium ion cells has been required every year. However, now the capacity of carbon anodes is getting closer to the theoretical value (372 mAh g^{-1}). Then, new anode materials having higher energy density than carbon have been studied. Examples of these materials are lithium metal, various Si-based and Sn-based compounds [1]. At this stage, the cycleability of these materials is not sufficient for commercial use. The choice of the electrolyte materials (solvents and solutes) is one of the most important factors for the charge–discharge cycling performance of lithium cells with various anodes.

Many researches on the electrolyte solutions have been carried out for improving lithium cycleability [2]. One of these researches is to modify and stabilize the chemical structure of carbonate solvents by introducing fluorine atoms. Examples of these solvents are fluoro-cyclic carbonates such as fluoro-EC, fluoro-propylene carbonate and fluoro-linear carbonates such as fluoro-methylacetae, fluoro-ethylmethyl carbonate, fluoro-diethyl carbonate, fluoro-dimethyl carbonate [3–5]. Also, various additives for electrolyte solutions have been studied. Typical example is vinylene carbonate (VC). VC has high reduction potential and forms a good surface film on anodes such as lithium metals and carbons for the improvement of cycling efficiency [6].

In our previous work, influence of poly-ether modified siloxanes as electrolyte additives to $LiPF_6$-EC/EMC on lithium cycling efficiency has been reported [7]. Lithium cycling efficiencies improved and an impedance of anode/electrolyte interface decreased by adding poly-ether modified siloxanes. These compounds are less reactive toward lithium and adsorbed on the lithium anode surface. This adsorption layer suppresses the lithium dendrite formation and the reduction of electrolyte solutions by lithium [7]. This mechanism is similar to an addition of surfactants (surface active agents) to electrolyte solutions such as poly-ethyleneglycol dimethyl ethers [8]. However, there may be a problem from a practical point of view. That is a small solubility of $LiPF_6$ in poly-ether modified siloxanes.

In this study, influence of carbonate-modified siloxanes as co-solvent of mixed solvent electrolytes on lithium cycling efficiency was examined. As the base electrolyte solution, 1 M (M: mol L^{-1}) $LiPF_6$-EC/MEC (3:7 in volume mixing ratio) was used. As the anodes, lithium metal was investigated. As carbonate-modified siloxanes, 4-(2-trimethylsilyloxydimethylsilylethyl)-1,3-dioxolan-2-one (sample A) and 4-(2-bis(trimethylsilyloxy)methylsilylethyl)-

* Corresponding author. Tel.: +81 277 30 1382; fax: +81 277 30 1380.
E-mail address: tobi@chem-bio.gunma-u.ac.jp (S.-i. Tobishima).

0378-7753/$ – see front matter © 2009 Elsevier B.V. All rights reserved.
doi:10.1016/j.jpowsour.2009.07.042

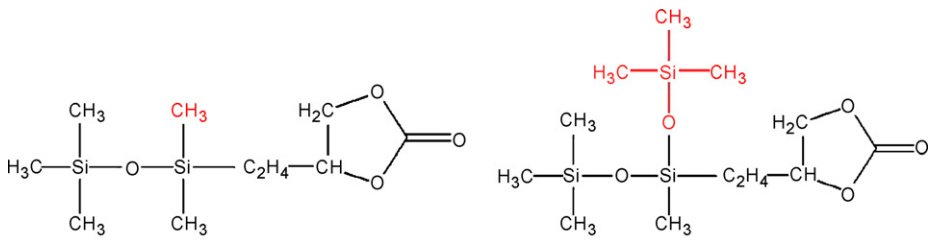

Fig. 1. Chemical structure of carbonate-modified siloxanes, sample A: 4-(2-trimethylsilyloxydimethylsilylethyl)-1,3-dioxolan-2-one and sample B: 4-(2-bis(trimethylsilyloxy)methylsilylethyl)-1,3-dioxolan-2-one.

1,3-dioxolan-2-one (sample B) were investigated. Fig. 1 shows the chemical structure of two siloxanes used in this work. These siloxanes are derivatives of butylene cyclic carbonate or vinyl ethylene carbonate. Chemical bonding of Si–O is stronger and more stable than that of C–O. They are colorless and clear liquid at room temperature. Their viscosities are 18.0×10^{-3} N m^{-2} for sample A and 22.5×10^{-3} N m^{-2} for sample B at 20 °C, respectively. These values are higher than that of EC/EMC (3:7 in volume mixing ratio) (1.18×10^{-3} N m^{-2}).

2. Experimental

2.1. Preparation of electrolyte solutions

Siloxanes were obtained from Shin-Etsu Chemical Co. Electrolyte solutions were prepared by mixing 1 M $LiPF_6$, EC/MEC (3:7 in volume ratio) (Tomiyama Pure Chemicals Co., Lithium Battery Grade) and siloxanes. Before mixing, siloxanes were dried over molecular sieves 3A (Kanto Chemicals Co.). Water content of electrolyte solutions was less than 20 ppm as determined by the Karl–Fisher titration method. Hereafter, "EM" represents 1 M $LiPF_6$-EC/MEC (3:7) and "EM + sample A 30 vol.%" represents 1 M $LiPF_6$-EC/MEC (3:7) (70 vol.%) + sample A (30 vol.%).

2.2. Charge–discharge cycling tests of lithium anodes and $LiCoO_2$ cells

Cyclic voltammetry was performed, using a glass cylindrical test cell with a lithium metal sheet counter electrode (0.1 mm thickness) pressed on a Ni net (200 mesh, 15 mm length, 4 mm width, 0.05 mm thickness) and a Pt working electrode (4 mm length, 4 mm width and 0.05 mm thickness, 0.09 cm^2). Lithium charge–discharge cycling tests were carried out galvanostatically, using a coin cell (coin type 2032, diameter 20 mm in diameter, 3.2 mm in thickness) with a lithium metal sheet counter electrode (0.1 mm thickness, 15 mm diameter) and a stainless steel (SUS 316) cathode case of the coin cell as the working electrode. The charge–discharge cycling efficiency (Eff) was obtained from the ratio of the stripping charge (Qs)/plating charge (Qp) on the stainless steel electrode with a charge–discharge voltage range of −2.0 V to 1.0 V. The charge–discharge current density (Ips) was 0.5 mA cm^{-2}. The Qp had a constant value of 0.88 mAh cm^{-2}.

In cases of natural graphite electrodes, the charge–discharge tests were carried out by the charge–discharge voltage cut-off (0 V and 1.5 V vs. Li/Li$^+$) with a constant current density of 0.5 mA cm^{-2} by using the 2032 coin cells. These cells have a lithium metal counter electrode and the working electrode of graphite. Using the 2032 coin cells carried out the charge–discharge test of $LiCoO_2$/Si–SiO_2–carbon composite (Si–C) cells.

For these experiments, we prepared the printed carbon electrodes by coating a Ni sheet with a mixture of carbon powder (around 18 mg) and poly(vinylidene fluoride) (PVDF) (weight ratio of carbon: PVDF = 9:1) in N-methyl pyrolidinone (NMP). We then evacuated the solvent and dried the electrodes. The printed carbon electrodes are 15 mm in diameter and 0.15 mm in thickness. Natural graphite powder used here has an average particle size of 10.7 μm in diameter, a surface area of 10.3×10^3 m kg^{-1} and a density of 0.21 kg m^{-3}. The printed $LiCoO_2$ electrodes (15 mm in diameter and 0.15 mm in thickness) were prepared by coating an Al sheet with a mixture of $LiCoO_2$ (around 50 mg), acetylene black (AB, conductive carbon) and PVDF (weight ratio of $LiCoO_2$:AB:PVDF = 85:5:10) in NMP. We then evacuated the solvent and dried the electrodes.

The printed Si–C electrodes (15 mm in diameter and 0.15 mm in thickness) were prepared by similar method as natural carbon electrodes by using Si–C powder and polymer binder. Si–C material was prepared according to the papers [9–11] by methane–argon gas mixture-chemical vapor deposition (CVD) with 1100 °C heat treatment. Image of this final product of Si–C material is shown in Fig. 2. Fine silicon crystal was distributed in the SiO_2. The surface of the final product was covered with double layers composed of thin inside layer of silicon carbide (SiC) and thick outside layer of carbon.

All the electrochemical measurements were carried out at 25 °C.

2.3. Thermal stability tests of electrolyte solutions

Thermal behavior of the electrolyte solutions toward C_6Li_x was evaluated with a differential scanning calorimeter (DSC, Rigaku Co., model TAS-100) and a crimp-sealed stainless steel pan. In the thermal stability tests of the electrolyte solutions toward C_6Li_x, the DSC sample was composed of about 7 mg of carbon and 3 μl of electrolyte. All the DSC experiments were carried out at a heating rate of 10 °C min^{-1} from room temperature to 450 °C. As described above, C_6Li_x was prepared by charge–discharge of the 2032 Li/natural graphite cells.

2.4. AC impedance and conductivity measurements

The AC impedance measurements of lithium/electrolyte interface were carried out by using Li/SUS coin cells with an impedance analyzer (Iviumstat, Hokuto Denko Co.). AC frequency range was 100 mHz to 20 kHz and amplitude of vibration was 20 mV. Conduc-

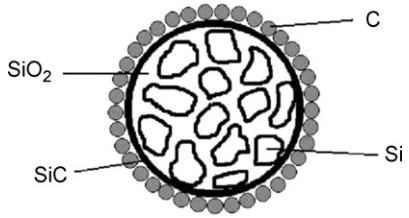

Fig. 2. Image of Si–SiO_2–carbon composite (Si–C).

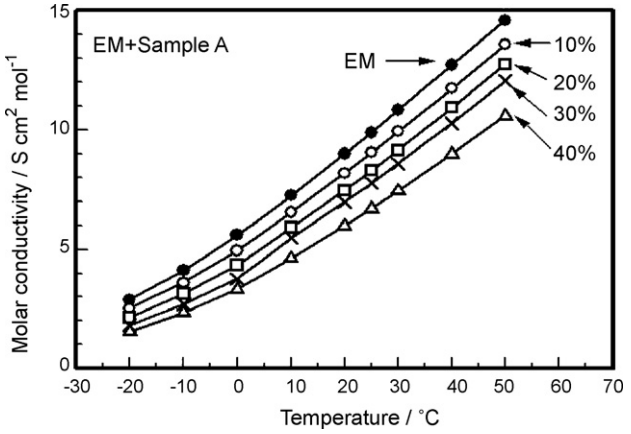

Fig. 3. Relationship among molar conductivity, mixing ratio of siloxane and temperature for EM + siloxane (sample A).

tivity of electrolyte solutions was measured using symmetry cell with platinum black electrodes at 1 kHz AC impedance. Viscosity of the electrolyte solution was measured with an Ostwald viscometer.

3. Results and discussion

3.1. Electrolyte conductivity

Fig. 3 shows the relationship between molar conductivity, mixing volume ratio of siloxane and temperature for EM + siloxane (sample A) ternary mixed solvent electrolytes. Fig. 4 shows the conductivity of EM + siloxane (sample B). With an increase in siloxane content, conductivities tended to decrease. As the temperature increases, conductivities tended to increase. At 20 °C, EM showed the conductivity of 8.9 S dm^2 mol^{-1} while EM + sample A (40 vol.%) showed 5.9 S dm^2 mol^{-1} and EM + sample B (60 vol.%) showed 4.7 S dm^2 mol^{-1}. These conductivity behaviors may be explained as the follows. Conductivity is proportional to the product of number of free ions (degree of ionic dissociation of the solute) and ion migration speed. Dielectric constant and ion radius affect the degree of ionic dissociation degree. The viscosity of the solvents fundamentally affects ion migration speed. $LiPF_6$ has relatively large anion radius among well-known lithium salts used for lithium batteries. For instance, anion radius of PF_6^- (0.254 nm) is larger than those of ClO_4^- (0.237 nm) and BF_4^- (0.229 nm) [12]. Then, $LiPF_6$ itself has relatively high ionic dissociation degree. However, large anion leads to lower migration speed. Figs. 5 and 6

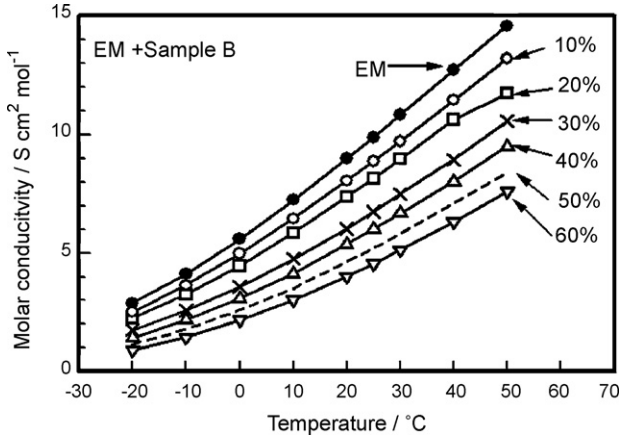

Fig. 4. Relationship among molar conductivity, mixing ratio of siloxane and temperature for EM + siloxane (sample B).

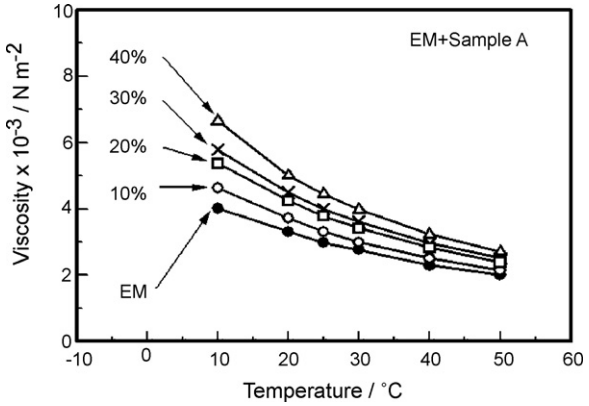

Fig. 5. Relationship among viscosity, mixing ratio of siloxane and temperature for EM + siloxane (sample A).

show the viscosity of EM + sample A and EM + sample B, respectively. With an increase in siloxane content, viscosity increases, because siloxane has higher viscosity than that of EM. So, viscosity affects the conductivity more strongly than dielectric constant in case of $LiPF_6$-EM + siloxanes. With an increase in temperature, conductivity increases. This phenomenon also arises from the influence of the viscosity, because both the viscosity and dielectric constant increase with a reduction in temperature [13].

3.2. Charge–discharge cycling properties of lithium metal anodes in the electrolyte solutions with siloxanes

Cyclic voltammetry (cv) of lithium metal (Li) in EM + siloxanes was carried out by using a glass cell consisted of Li counter and Pt working electrodes. Fig. 7 shows the cv results of Li at first cycle in EM alone and EM + siloxanes (sample A). Fig. 8 shows the cv results of Li at first, 10th and 30th cycle in EM + siloxanes (sample A, 10 vol.%). The following three results were obtained. (i) Lithium was able to charge and discharge in EM + siloxanes, (ii) Li charge–discharge capacity depended on the addition amounts of siloxanes, and (iii) Li charge–discharge capacities in EM + siloxanes tended to be larger than that in EM alone.

Next, using a coin cell consisted of Li anode and SUS cathode, charge–discharge cycling tests of lithium in EM + siloxanes were carried out. Charging capacity was 0.88 mAh cm^{-2}. Figs. 9 and 10 show charge–discharge cycling test results of Li anodes in EM + siloxanes (sample A) and in EM + siloxanes (sample B), respectively. Fig. 11 show average lithium cycling efficiencies from first to 30th cycle ($Eff_{Ave.30}$) in EM + siloxanes (sample A) and in EM + siloxanes (sample B). Values of $Eff_{Ave.30}$ in EM + siloxanes were

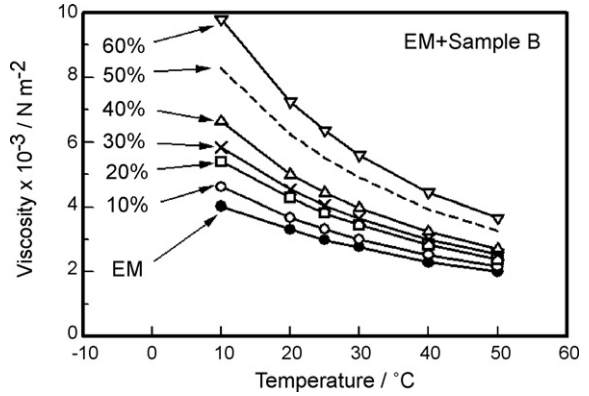

Fig. 6. Relationship among viscosity, mixing ratio of siloxane and temperature for EM + siloxane (sample B).

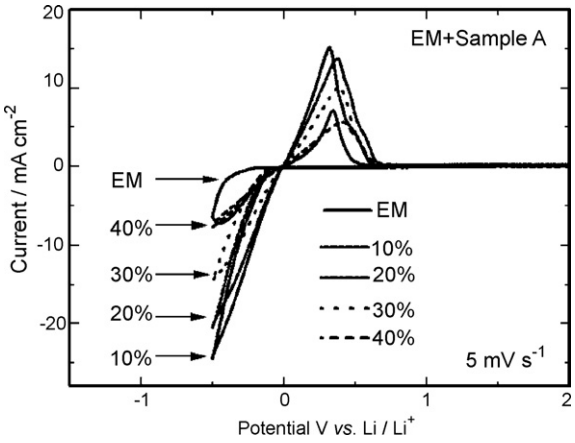

Fig. 7. Cyclic voltamgram of lithium in EM + siloxane (sample A) at first cycle, Pt working electrode, scanning rate: 5 mV s^{-2}, −0.5 V to 2.0 V vs. Li/Li^+.

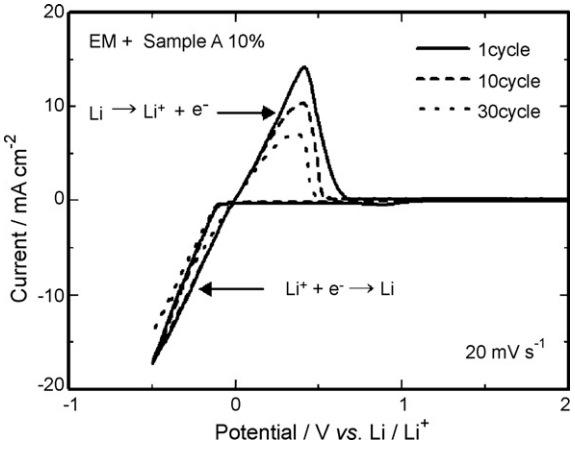

Fig. 8. Cyclic voltamgram of lithium in EM + siloxane (sample A) at first, 10th and 30th cycle, Pt working electrode, scanning rate: 20 mV s^{-2}, −0.5–2.0 V vs. Li/Li^+.

higher than that in EM alone. $Eff_{Ave.30}$ exhibited the maximum value at 40 vol.% mixing amount for sample A and at 60 vol.% for sample B, respectively. $Eff_{Ave.30}$ values were as high in the order of sample B > sample A > EM.

From the charge–discharge test results, it was found that the addition of siloxanes was effective for the improvement of cycling efficiency of lithium metal anodes.

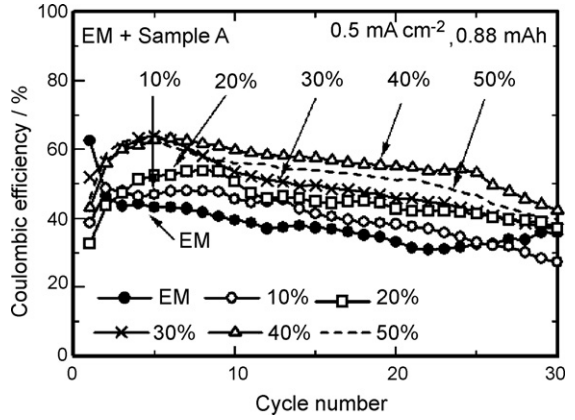

Fig. 9. Charge–discharge cycling tests results of lithium in EM + siloxane (sample A), SUS working electrode, Ips = 0.5 mA cm^{-2}, Qp = 0.88 mAh cm^{-2}, charge–discharge cut-off voltages: −2.0 V and 1.0 V vs. Li/Li^+.

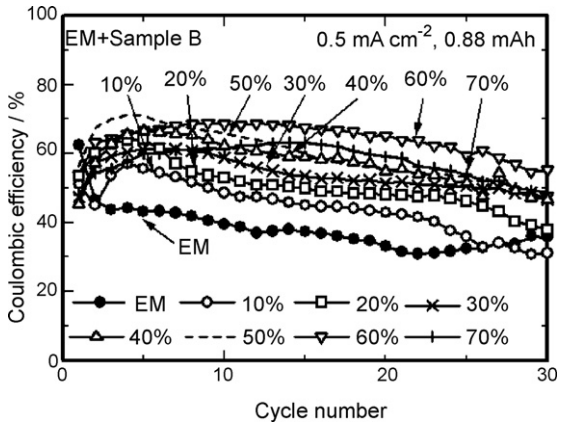

Fig. 10. Charge–discharge cycling tests results of lithium in EM + siloxane (sample B), SUS working electrode, Ips = 0.5 mA cm^{-2}, Qp = 0.88 mAh cm^{-2}, charge–discharge cut-off voltages: −2.0 V and 1.0 V vs. Li/Li^+.

3.3. AC impedance measurement results for interface between lithium electrode and electrolyte solutions

In organic electrolyte solutions, the surface of lithium is covered with thin film after charge–discharge cycling [14]. This surface film is formed by the reduction of electrolyte solution by lithium. This film is generally known as the solid electrolyte interface (SEI) [15]. The SEI is consisted of several chemical compounds such as alkyl lithium carbonate [14]. During charge and discharge, lithium ion must diffuse in the SEI. In many cases, this diffusion process is considered to be a rate-determining step for electrochemical reaction. To investigate the charge–discharge behavior of Li in EM + siloxanes in more detail, the AC impedance measurements of lithium/electrolyte interface were carried out by using Li/SUS coin cells. Before AC measurements, lithium was electrochemically plated on the SUS cathodes. Namely, the impedance measurements were carried out for the cells of Li/Li plated on SUS.

Fig. 12 shows the Cole–Cole plot of Li/Li cells after first charge (plating Li on SUS) in 1 M $LiPF_6$-EM + siloxanes. Impedance measurements were carried out just after the end of first charge. The impedance values of electrolyte solutions of EM + siloxanes (both samples A and B) were larger than EM alone by an increase in viscosity as already explained in Section 3.1. After first charge, impedance values of the electrolyte/Li interface in EM + siloxanes were smaller than that in EM alone. These results suggest that the impedance of the surface film or layer of lithium in EM + siloxanes is smaller than

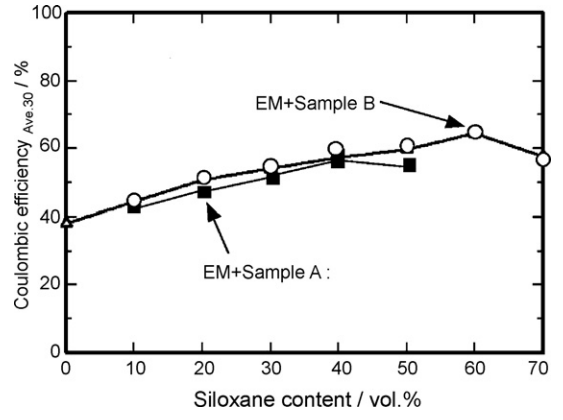

Fig. 11. Relationship between siloxane content and average lithium cycling efficiency (coulombic $efficiency_{Av.30}$), EM + siloxanes (samples A and B), SUS working electrode, Ips = 0.5 mA cm^{-2}, Qp = 0.88 mAh cm^{-2}, charge–discharge cut-off voltages: −2.0 V and 1.0 V vs. Li/Li^+.

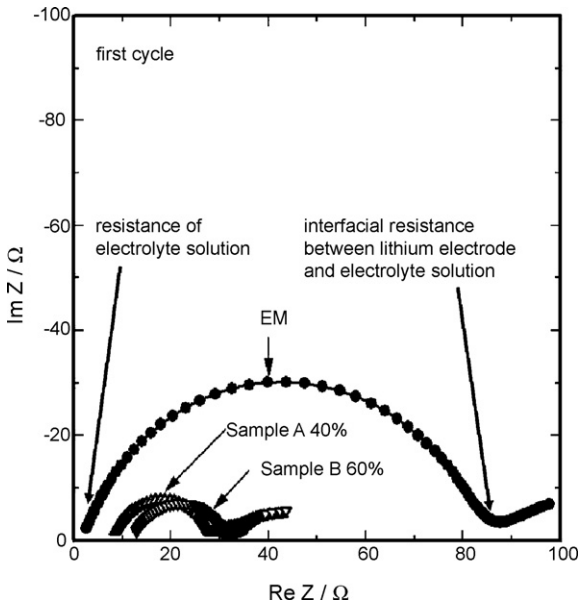

Fig. 12. Cole–Cole plot of Li/electrolyte interface, Li/Li cells, EM + sample A or sample B after first charge at 25 °C, Ips = 0.5 mA cm^{-2}, Qp = 0.88 mAh cm^{-2}, charge–discharge cut-off voltages: −2.0 V and 1.0 V vs. Li/Li$^+$.

that in EM alone. Fig. 13 shows the Cole–Cole plot of Li/Li cells after 30th charge. Also, after 30th cycle, impedance values of the electrolyte/Li interface in EM + siloxanes were smaller than that in EM alone. These results suggest that the electrode/electrolyte interface in EM + siloxanes is different from that in EM alone.

Figs. 14 and 15 show a dependency of the impedance after first charge on temperature. With an increase in temperature, the impedance values both in EM and in EM + siloxanes decreased. Between 0 °C and 50 °C, the impedance values in EM + siloxanes were lower than those in EM alone.

Fig. 16 shows the relationship between the resistance of lithium/electrolyte solution interface after first charge and storage duration at 25 °C. In case of EM alone, impedance tended to increase

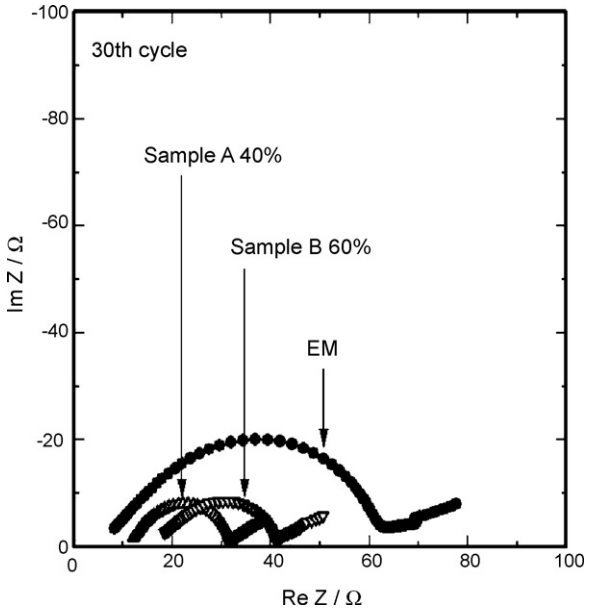

Fig. 13. Cole–Cole plot of Li/electrolyte interface, Li/Li cells, EM + sample A or sample B after 30th charge at 25 °C, Ips = 0.5 mA cm^{-2}, Qp = 0.88 mAh cm^{-2}, charge–discharge cut-off voltages: −2.0 V and 1.0 V vs. Li/Li$^+$.

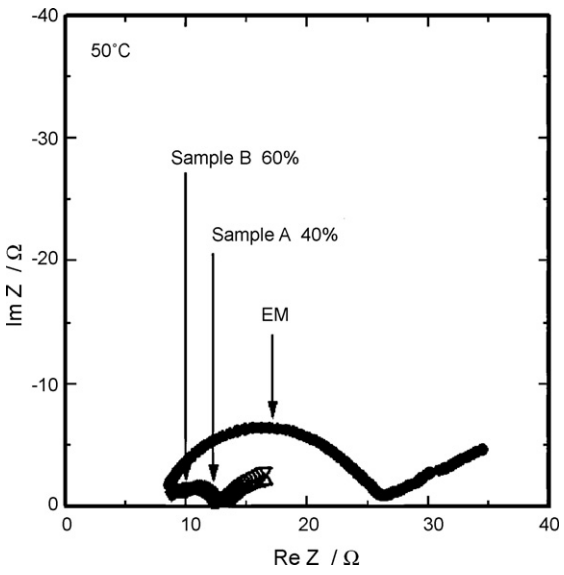

Fig. 14. Cole–Cole plot of Li/electrolyte interface, Li/Li cells, EM + sample A or sample B after first charge at 60 °C.

with an increase in storage duration. This result indicates the gradual growth of surface film of electrode by chemical reaction in EM alone. However, in case of EM + siloxanes, the degree of increase in impedance with an increase in storage duration was considerably lower than that in EM alone. These results suggest addition of siloxanes lead the suppressing the electrolyte reduction by the change in structure of interface between lithium electrode and electrolyte solutions.

To investigate the reactivity between Li and the electrolyte solutions, linear potential sweep measurements in the cathodic direction were carried out by using Li/SUS coin cells (Fig. 17). Both in EM alone and EM + siloxanes, large cathodic currents began to flow around −0.9 V vs. Li/Li$^+$. These currents correspond to Li plating. These cathodic reactions of Li plating have more than 0.9 V polarization (overpotential) toward thermodynamic equilibrium potential of Li/Li$^+$ (0 V). Before Li plating, relatively smaller cathodic currents flow between −0.15 V and −0.9 V vs. Li/Li$^+$. These currents corre-

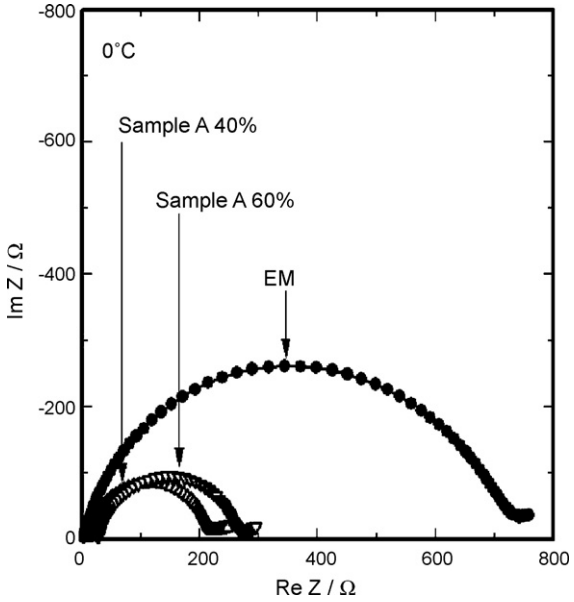

Fig. 15. Cole–Cole plot of Li/electrolyte interface, Li/Li cells, EM + sample A or sample B after first charge at 0 °C.

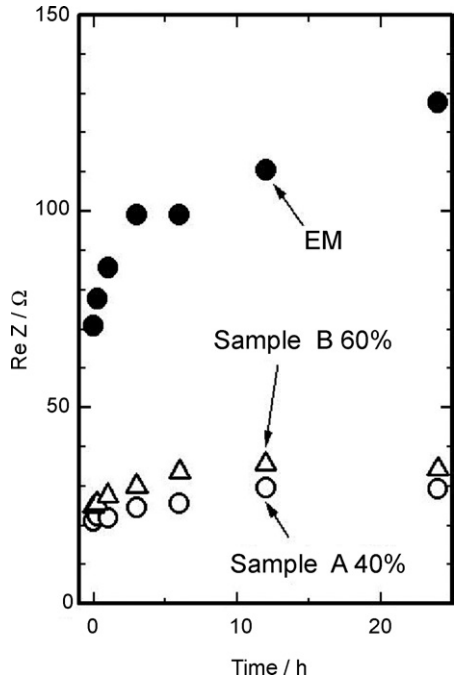

Fig. 16. Relationship between the resistance of Li/electrolyte interface and storage duration at 25 °C after first charge, Ips = 0.5 mA cm^{-2}, Qp = 0.88 mAh cm^{-2}, charge–discharge cut-off voltages: −2.0 V and 1.0 V vs. Li/Li$^+$.

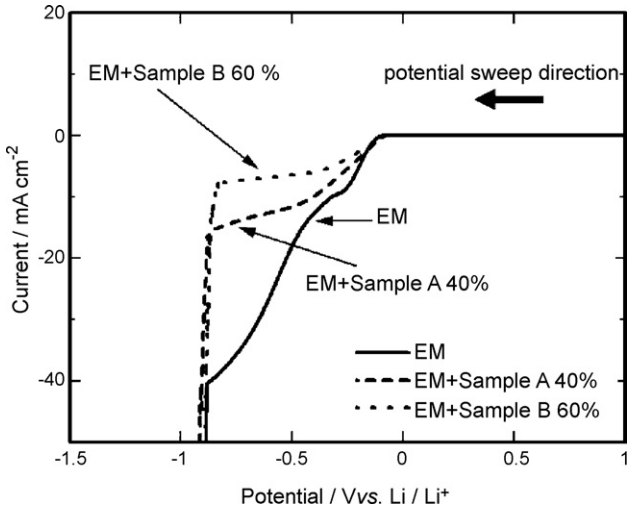

Fig. 17. Linear potential sweep results of EM + sample A or sample B, cathodic scan, scanning rate:1 mV s^{-1}, sweeping from 1.0 V to −1.0 V vs. Li/Li$^+$.

spond to the reduction (cathodic reaction) of EM. In EM + siloxanes (samples A and B), these currents between −0.15 V and −0.9 V became smaller than that in EM alone. So, the addition of siloxanes (samples A and B) is effective on suppressing the electrolyte reduction.

After one cycle of the charge–discharge of Li/natural graphite coin cells (2032 type) with EM + siloxane (sample A or sample B, 10 vol.%), solid compounds formed on the surface of carbon electrode were analyzed by ESCA. By mixing siloxanes, content of oxygen tended to increase and carbon tended to decrease. These results suggest the change in chemical composition of anode surface film. Unfortunately, it was not clear whether the surface solid compounds contain silicon atoms or not.

3.4. Model for interface between lithium electrode and electrolyte solutions

Summarizing the results of lithium cycling efficiency measurements by cv and coin cells, impedance measurements and electrolyte reduction behavior, the following mechanism may be proposed for the improvement of lithium cycling efficiency by addition of siloxanes. Fig. 18 shows the proposed models for the Eff enhancement by adding siloxanes. Just after charging (lithium

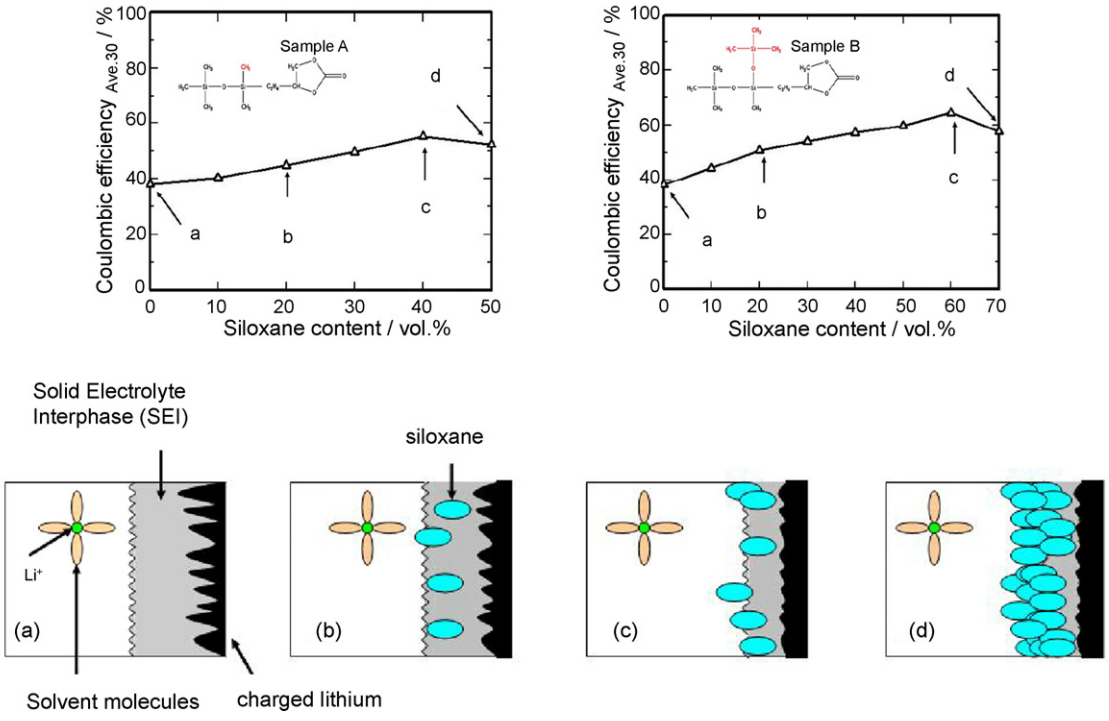

Fig. 18. Proposed mechanism for change in lithium cycling efficiency in EM + siloxanes.

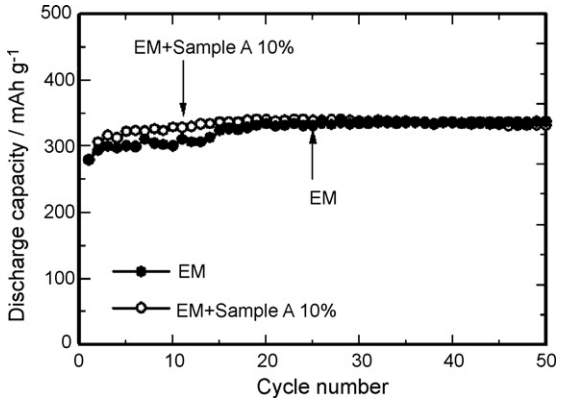

Fig. 19. Charge–discharge cycling tests results of natural graphite/Li cells with EM + siloxane (sample A, 10 vol.%), Ips = 0.5 mA cm^{-2}, charge–discharge cut-off voltages: 0 V and 1.5 V vs. Li/Li$^+$.

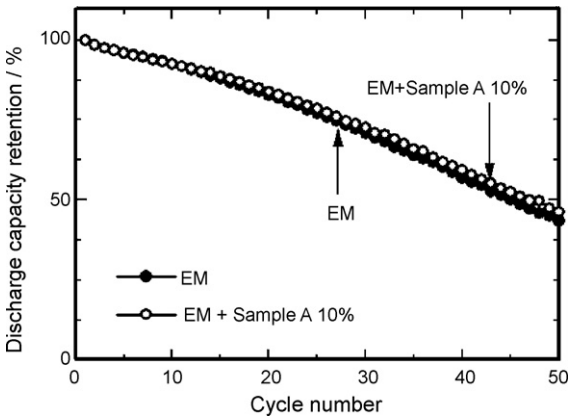

Fig. 20. Charge–discharge cycling test results of Si–C/$LiCoO_2$ cells with EM + siloxane (sample A, 10 vol.%), Ips = 0.5 mA cm^{-2}, charge–discharge cut-off voltages: 4.0 V and 2.5 V.

deposition), freshly deposited lithium is chemically active. On the lithium surface, EM is chemically reduced by lithium and produces the surface film. The reduction products were reported to be solid compounds and gas compounds [14]. The solid compounds remained on the lithium produce the SEI. Fig. 18(a): By no addition of siloxane, the surface film is composed of reduction products of EM. Fig. 18(b): By the small addition of siloxane, the surface film is mainly composed of reduction products of EM. Small amounts of siloxane is involved in the SEI or it adsorbs on the SEI surface. Siloxanes are less reactive than EM. Fig. 18(c): By the medium amounts of siloxane (40 vol.% for sample A and 60 vol.% for sample B), the surface film is thin and is composed of both the reduction product of EM and siloxane. Fig. 18(d): By adding larger amounts of siloxane, the excess and thick siloxane layer exists around the lithium electrode. This excess siloxane could be resistive for the smooth charge–discharge of lithium (lithium ion diffusion). Then, the Eff improves by adding siloxanes and shows the maximum value against the addition amounts of siloxanes.

3.5. Charge–discharge cycling properties of lithium in graphite anodes in electrolyte solutions with siloxanes

Fig. 19 shows the charge–discharge cycling test results of natural graphite electrodes in EM + siloxane (sample A) by using Li/graphite coin cells. Discharge capacity density (mAh g^{-1}) in *y*-axis of Fig. 19 is calculated based on graphite active material weight. Discharge capacity is the capacity of the lithium deintercalated from graphite electrodes. Stability of discharge capacity densities with cycling in EM + siloxane was slightly better than that in EM alone.

3.6. Charge–discharge cycling properties of Si–C anode/$LiCoO_2$ cells with siloxane electrolytes

Fig. 20 shows the charge–discharge cycling test results of Si–C/$LiCoO_2$ cells with EM + sample A. In Fig. 2, the discharge capacity at first cycle is defined as 100% retention. Slightly better cycling performance in EM + siloxane (sample A) than in EM alone was obtained. 100% retention corresponds to 130 mAh g^{-1} of the discharge capacity density based on $LiCoO_2$ weight and 2200 mAh g^{-1} of the discharge capacity density based on Si–C weight. The capacity density of $LiCoO_2$ in EM + siloxane was almost the same as that in EM alone. The capacity density of Si–C anodes in EM + siloxane was slightly larger than in EM alone. Utilization of Si–C anode is expected to improve by adding siloxane. So, by optimizing the charge–discharge cut-off voltages and the balance ratio of anode and cathode in the cell, the cycling performance may improve more.

3.7. Thermal stability tests of electrolyte solutions with siloxanes

Thermal stability of the electrolytes is important for the cell safety [9,10]. DSC measurements were carried out to investigate the reaction behavior of electrolyte solutions and lithium. In the latter test, instead of lithium metal, graphite–lithium (C_6Li_x) was used.

Fig. 21 shows the DSC results for C_6Li_x with electrolytes. C_6Li_x was prepared by charge–discharge of Li/graphite coin cell. Charge–discharge cycling was carried out twice between 0 V and 1.5 V at 0.5 mA cm^{-2}. Chemical composition of obtained product is $C_6Li_{0.85}$.

In case of $C_6Li_{0.85}$ with EM alone, two heat generation regions were observed. The first heat-output was mild and started at 130 °C. It continued until a sharp exothermic peak appeared around 280 °C. A possible mechanism for these DSC results is as follows [16]. The first mild heat-output corresponded to the reduction of EM by the lithium inside the carbon. This reaction has already occurred at first charge and produced the SEI film on the carbon surface at room temperature. At 130 °C, the PVDF, electrode binder, swells. Then, the carbon that is not covered with SEI appears, and the lithium inside the carbon reacts with the electrolyte solution [16]. SEI is consisted of several chemical materials. Another possibility as the cause for first heat-output is suggested to be the decomposition of the part of SEI compounds [17] or the conversion of metastable SEI components to stable SEI components [18]. At 280 °C, the surface SEI film is broken. Almost the whole of carbon surface appears,

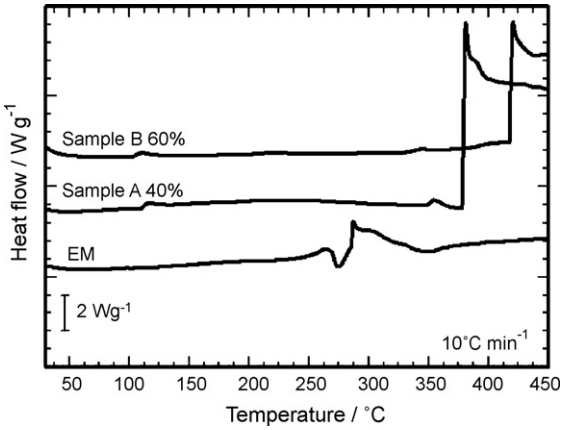

Fig. 21. DSC results of EM + siloxane (sample A or sample B) with $C_6Li_{0.85}$, scanning rate: 10 °C min^{-1}.

and the lithium in the carbon reacts vigorously with the electrolyte solution [16].

In case of $C_6Li_{0.85}$ with the EM + siloxane (sample A or sample B), two small heat-output were observed at 100 °C and 220 °C. These heat-output may be introduced from the reduction of electrolyte solutions by lithium inside the carbon, because a part of liquid state siloxanes fluids from the SEI film capturing siloxanes with an increase in temperature. Temperature starting large heat-output shifted from 280 °C to higher temperature of 360 °C for EM + sample A and 420 °C for EM + sample B, respectively.

So, unfortunately the addition of carbonate-modified siloxanes was not completely effective on the improvement of thermal stability.

4. Conclusion

Charge–discharge cycling efficiencies of, lithium metal improved by adding carbonate-modified siloxanes to EM. The impedance of anode/electrolyte interface decreased by adding siloxanes. Slightly better cycling behavior of natural graphite anode was obtained by adding siloxanes. Si–C/$LiCoO_2$ cells exhibited better anode utilization and good cycling performance by using 1 M $LiPF_6$-EC/MEC + siloxane electrolytes. DSC results for graphite–lithium anodes with electrolyte solutions indicated that amount of heat-output did not decrease while the temperature starting the large heat-output shifted to higher temperature about 100 °C by adding siloxanes. By modifying chemical structure of siloxanes, we expect to obtain the more improvement of charge–discharge cycling performance and thermal stability of lithium cells.

References

[1] N. Tamura, R. Ohshita, M. Fujimoto, M. Kamino, S. Fujitani, J. Electrochem. Soc. 150 (2003) A679.
[2] L.A. Dominey, in: G. Pistoia (Ed.), Lithium Batteries, Elsevier, The Netherlands, 1994 (Chapter 4).
[3] R. McMillan, H. Slegr, Z.X. shu, W. Wang, J. Power Sources 81–82 (1999) 20.
[4] J. Yamaki, I. Yamazaki, M. Egashira, S. Okada, J. Power Sources 102 (2001) 288.
[5] M. Ihara, B.T. hang, K. Sato, M. Egashira, S. Okada, J. Yamaki, J. Electrochem. Soc. 150 (2009) A1476.
[6] M. Ue, Extended Abstracts of the Battery and Fuel Cell Materials Symposium, Gratz, Austria, 2004, p. 53.
[7] T. Inouse, S. Tada, H. Morimoto, S. Tobishima, J. Power Sources 161 (2006) 550.
[8] M. Mori, Y. Narukawa, K. Naoi, D. Futeux, J. Electrochem. Soc. 145 (1998) 2340.
[9] M. Miyachi, H. Yamamoto, H. Kawai, T. Ohta, M. Shirakawa, Extended Abstracts of 206th Electrochemical Society Meeting, Abs. No. 311, 2004.
[10] T. Morita, N. Takami, Extended Abstracts of 206th Electrochemical Society Meeting, Abs. No. 312, 2004.
[11] Jpn. Kokai Tokkyo Koho (Jpn. patent application), JP2004-47404A (2004).
[12] M. Ue, J. Electrochem. Soc. 141 (1994) 3336.
[13] W. Biltz, W. Fischer, Z. Phys. Chem. (Leipzig) 151A (1930) 12.
[14] D. Aurbach, E. Granot, Electrochim. Acta 42 (1997) 697.
[15] E. Peled, D. Golodnitsky, J. Pencier, in: J.O. Besenhard (Ed.), Handbook of Battery Materials, Wiley–VCH, Germany, 1999 (Chapter 6).
[16] J. Yamaki, H. Takatsuji, T. Kawamura, M. Egashira, Solid State Ionics 148 (2002) 241.
[17] A. Du Pasquier, F. Disma, T. Bowmer, A.S. Gozdz, G. Amatucci, J.M. Tarascon, J. Electrochem. Soc. 145 (1998) 472.
[18] M.N. Richard, J.R. Dahn, J. Electrochem. Soc. 146 (1999) 2068.